

**Kinetic energy control in action-derived molecular dynamics simulations**In-Ho Lee,<sup>1,\*</sup> Jooyoung Lee,<sup>2</sup> and Sangsan Lee<sup>3</sup><sup>1</sup>*Korea Research Institute of Standards and Science, Daejeon 305-600, Korea*<sup>2</sup>*Korea Institute for Advanced Study, Seoul 130-012, Korea*<sup>3</sup>*Korea Institute of Science and Technology Information, Yusong-ku, P.O. Box 122, Daejeon, Korea*

(Received 17 August 2002; revised manuscript received 28 February 2003; published 21 August 2003)

We present a computational approach to obtain classical atomic trajectories for given initial and final atomic configurations. By introducing an additional penalty function to the action of Passerone and Parrinello [Phys. Rev. Lett. **87**, 108302 (2001)] the quality of atomic trajectories is greatly improved in terms of the Onsager-Machlup action. We demonstrate that this variant of the action is useful for improving path quality and consequently for atomic trajectory annealing. We utilize the one-way multigrid method as an efficient relaxation method for the construction of trajectories. The implementation of the proposed approach to a general system is quite straightforward as in the case of ordinary molecular dynamics simulations, i.e., the only requirement is to evaluate the potential energy and the atomic forces.

DOI: 10.1103/PhysRevB.68.064303

PACS number(s): 82.20.Wt, 02.70.Ns

**I. INTRODUCTION**

The process of concerted atomic rearrangement, despite its physical importance, is not fully understood in many cases. Molecular dynamics (MD) simulation technique is quite useful for the study of the time evolution of atomic systems.<sup>1</sup> However, conventional MD simulation approach fails to observe rare events where astronomically long simulations are required due to large activation energy barriers.<sup>2-10</sup> The time scales associated with rare events, such as configurational transitions of complex molecular systems, are many orders of magnitude longer than those of individual atomic vibration. To observe a rare event which takes place on the time scale of a second, it is necessary to simulate  $\sim 10^{15}$  MD steps since typical integration time in MD is in the range of a femtosecond. For this reason, the ordinary MD simulation approach is not a suitable method for the study of rare events in general.<sup>3-5</sup>

Significant progresses such as developments of activation-relaxation technique,<sup>8</sup> hyperdynamics,<sup>9</sup> parallel replica dynamics,<sup>11</sup> and dimer method<sup>12</sup> have been made for simulations of long-time events. In the activation-relaxation technique, the system is driven from one potential-energy basin to another by inverting the components of the force acting on the system. The new potential-energy basin is either accepted or rejected via Monte Carlo criteria. By introducing various structural changes in a condensed-matter system, it is possible to follow the reaction path as the configuration moves frequently from one basin to another. In the hyperdynamics simulation, the potential is modified by adding a bias potential term to raise the energy in the regions around the potential-energy basins. Correct equilibrium and dynamical properties are recovered by employing the time increment procedure based on the technique of importance sampling. Voter has developed the parallel replica dynamics<sup>11</sup> where many trajectories are simulated in parallel while waiting for structural transformations to occur. This method extends the time scale of a simulation in terms of its high parallel efficiency. Henkelman and Jónsson<sup>12</sup> have developed the dimer method which efficiently finds many saddle points. The

dimer method can be used for long time-scale simulations along with the kinetic Monte Carlo (MC) method, where the transition rate is approximated by the harmonic transition-state theory. For example, long time simulations of aluminum clusters on surface are carried out successfully using this approach.<sup>13</sup> It should be noted that, in these methods, the system is not guaranteed to reach the desired final configuration in the study of rare events.

When studying rare events, it is more appropriate to incorporate the given initial and final atomic configurations explicitly in the simulation, i.e., one formulates the problem into an action minimization problem with fixed boundary conditions: For given initial and final atomic configurations, one has to find the most probable path between the two states by optimizing a specially designed object function.<sup>2,3,14,15</sup> This approach is in contrast to the ordinary MD simulations where one has to wait indefinitely until the system with given initial configuration reaches the desired final state. To search the most probable path of the configurational change, one has to find the lowest saddle point connecting the two potential-energy basins corresponding to the initial and final states.

The nudged elastic band method, developed by Jónsson *et al.*<sup>6</sup> is a heuristic method to search for this saddle point, providing the activation barrier energy and the atomic configuration of the transition state. A similar method, string method, is also designed for the study of rare events.<sup>7</sup> However, these strategies do not take into account of dynamical conditions such as the total-energy conservation and the least action principle.

Recently, Passerone and Parrinello<sup>5</sup> proposed a powerful action-derived molecular dynamics (ADMD) method that explicitly determines the dynamical trajectory of an atomic system for given initial,  $\{\mathbf{R}(0)\}$  and final,  $\{\mathbf{R}(\tau)\}$  atomic configurations, and a chosen simulation time interval  $\tau$ .<sup>5</sup> This method was shown to be quite useful for the study of rare events. In ADMD simulations, one starts with an initial guess of the time trajectory connecting the given initial and final configurations. The final atomic trajectory is obtained by minimizing an appropriate action starting from the initial

guess. However, in practical application of the original ADMD method to a system, we observe that the final results of the atomic trajectories strongly depend on the initial guess of them.<sup>16</sup> In this paper, as a solution to this problem, we introduce an additional penalty function term to the original action. We show that, based on the measurement of the Onsager-Machlup action, the proposed action provides paths of significantly better quality compared to those from the original action. We also show that the ADMD method is superior to the nudged elastic band method in correctly estimating the activation energy barrier of a complex system.

The organization of the paper is as follows. In Sec. II, we summarize the original ADMD method by Passerone and Parrinello. In Sec. III, we present the extended action containing the control of kinetic energy. We also present the one-way multigrid approach as an efficient action minimization method. The summary and conclusion is provided in the final section.

## II. ORIGINAL ADMD METHOD AND THE QUALITY OF A TRAJECTORY

We are interested in a computational approach to find classical atomic trajectories to connect given initial and final atomic configurations. Atomic units ( $\hbar = m_e = e = 1$ ) are used throughout this paper. We look for classical atomic trajectories,  $\{\mathbf{R}_j\}$  of an  $N$ -atom conservative system with given potential energy,  $V(\{\mathbf{R}\})$ . The trajectories start at the point  $\{\mathbf{R}_{j=0}\} (= \{\mathbf{R}(0)\})$  at time  $t=0$  and finish at the point  $\{\mathbf{R}_{j=P}\} (= \{\mathbf{R}(\tau)\})$  at time  $t=\tau$ . An arbitrary atomic trajectory satisfying the boundary conditions can be represented by a straight line between the two points plus a series of sine functions as shown below:<sup>5,15</sup>

$$\mathbf{R}_j = \mathbf{R}(0) + \frac{j\Delta}{\tau} [\mathbf{R}(\tau) - \mathbf{R}(0)] + \sum_{k=1}^{P-1} \mathbf{a}_k \sin\left(\frac{k\pi j\Delta}{\tau}\right), \quad (1)$$

where  $\Delta (= \tau/P)$  is the discretized time interval and  $j$  ( $= 0, 1, 2, \dots, P$ ) is the time index. The sine expansion coefficient  $\mathbf{a}_k$  is composed of numbers bounded by a fixed amplitude  $A_{\max}$ . It is straightforward to obtain Fourier components of an atomic path represented by Eq. (1). It should be noted that, in the process of path relaxation (see Sec. III B), low-frequency components of a path relax more slowly than high-frequency ones. Therefore when performing path relaxation, it is convenient to start with low-frequency components of a path and move on by gradually adding high-frequency ones to accelerate the convergence.<sup>5</sup>

Passerone and Parrinello proposed an action,  $\Theta(\{\mathbf{R}_j\}, E)$  to generate an atomic trajectory for given sets of initial,  $\{\mathbf{R}(0)\}$ , and final,  $\{\mathbf{R}(\tau)\}$ , configurations.<sup>5</sup> The dynamical trajectory  $\{\mathbf{R}_j\}$  can be obtained by minimizing the following discretized action, mimicking the least action principle in the classical mechanics,

$$\Theta(\{\mathbf{R}_j\}, E) = \sum_{j=0}^{P-1} \Delta \left\{ \sum_{l=1}^N \frac{M_l}{2\Delta^2} (\mathbf{R}_j^l - \mathbf{R}_{j+1}^l)^2 - V(\{\mathbf{R}_j\}) \right\} + \mu \sum_{j=0}^{P-1} (E_j - E)^2. \quad (2)$$

Here the first term stands for a discretized classical action  $S$  of an  $N$ -atom system interacting by a given potential  $V(\{\mathbf{R}\})$ . The number of intermediate configurations between the two end points is set to  $P-1$ , and  $M_l$  is the atomic mass of atom  $l$ . The instantaneous total energy  $E_j$  at time step  $j$  is defined by<sup>5</sup>  $E_j = \sum_{l=1}^N (M_l/2\Delta^2) (\mathbf{R}_j^l - \mathbf{R}_{j+1}^l)^2 + V(\{\mathbf{R}_j\})$ . The initial and final configurations are fixed during the minimization of the action  $\Theta$ . The second part of the action  $\Theta$  is a penalty term, and the role of the parameter  $\mu$  is to control the value of the total energy of the system close to the target energy  $E$  along the path.<sup>5</sup>

Now, the problem is to find a solution  $\{\mathbf{R}_j\}$  which minimizes the discretized action  $\Theta(\{\mathbf{R}_j\}, E)$  for given  $E$ . In principle, rigorous application of a global optimization method such as the simulated annealing<sup>17</sup> should solve the problem. However, generally speaking, many global optimization problems are nontrivial, and we focus on a local minimization procedure in the present study.

In the ADMD simulation, it is important to check the quality of the resulting trajectory based on the fact that the trajectory satisfies the Newton's equation of motion, i.e., it follows closely the Verlet trajectory.<sup>2,3,5</sup> The key quantity for this measurement is the discretized Onsager-Machlup action,<sup>3,5</sup>

$$O = \sum_{l=1}^N \sum_{j=1}^{P-1} \left( 2\mathbf{R}_j^l - \mathbf{R}_{j-1}^l - \mathbf{R}_{j+1}^l - \frac{\Delta^2}{M_l} \frac{\partial V(\{\mathbf{R}_j\})}{\partial \mathbf{R}_j^l} \right)^2. \quad (3)$$

The trajectory of  $O=0$ , i.e., all the arguments in the parentheses become zero, is known as the Verlet trajectory.<sup>18</sup> The smaller the value of  $O$  is, the more closely the corresponding trajectory follows the Verlet trajectory. Therefore the quality of a trajectory is often measured<sup>3</sup> by the value of the Onsager-Machlup action  $O$  and we will adopt this in this work.

## III. RESULTS AND DISCUSSION

### A. Improved path quality

When performing the original ADMD simulation we often encounter a situation where the final converged trajectory depends strongly on the initial assignment of the expansion coefficients  $\{\mathbf{a}_k\}$ .<sup>16</sup> Here we illustrate this problem in a specific example, where we perform several ADMD simulations, using various sets of initial trajectories, of a Stone-Wales (SW) defect formation<sup>19</sup> in a  $C_{60}$  molecule.<sup>20,21</sup> A SW defect in a  $C_{60}$  is illustrated in Fig. 1, where the major configurational change is the  $90^\circ$  rotation of the two shaded carbons rearranging their neighboring bonds only. In this example, the problem is to find the most probable transition path connecting the initial configuration of the perfect

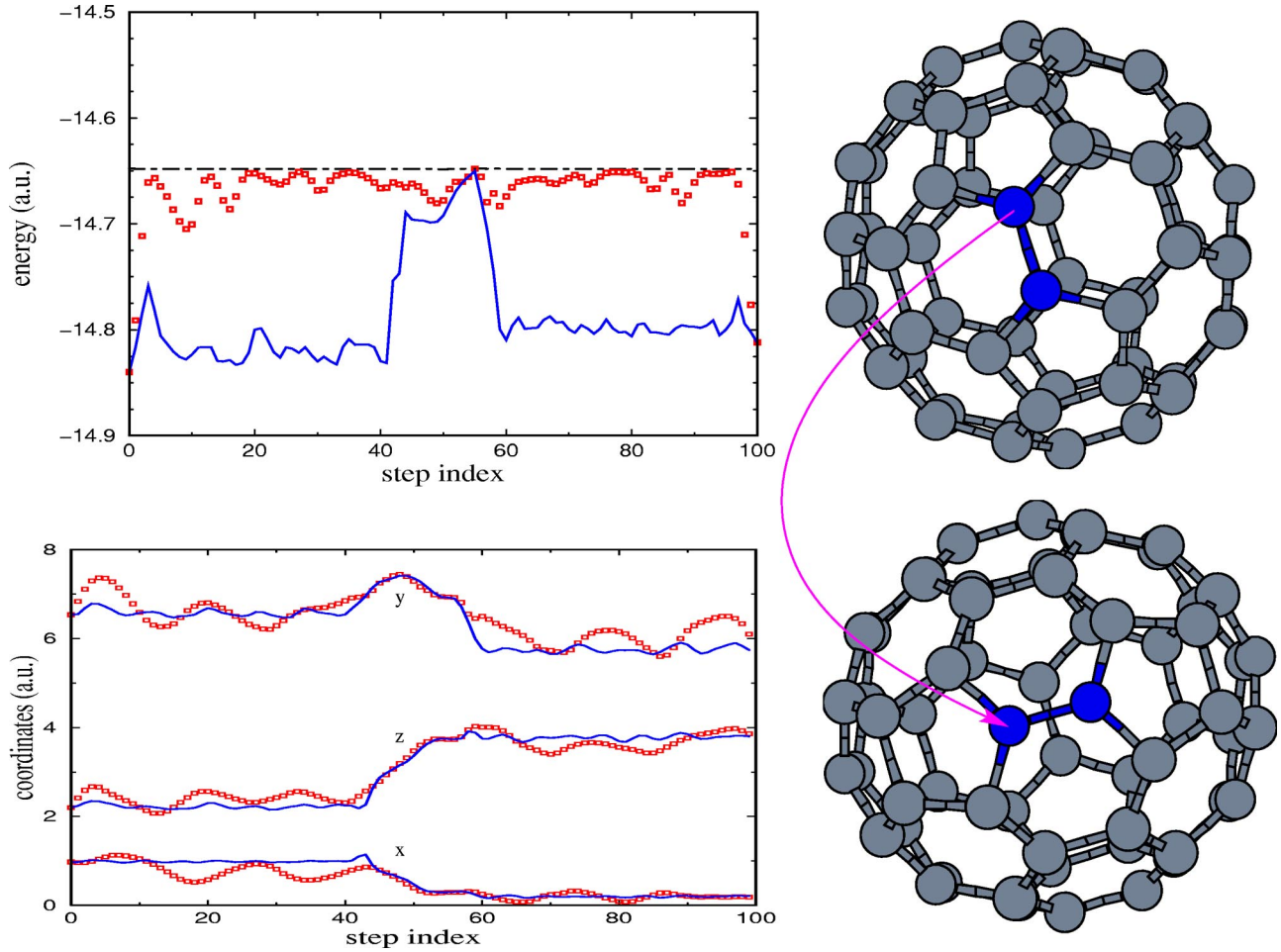


FIG. 1. An atomic trajectory associated with one out of two Stone-Wales defect atoms in the Stone-Wales transformation is shown. The initial and final configurations are shown at the right-hand side of the figure. Solid lines represent the potential energy and the atomic position along the path obtained by the current method, while symbols represent those by the Passerone and Parrinello's original method. Here we use  $\mu = 10^8$  a.u.,  $\nu = 10^{10}$  a.u., target variable  $T = 500$  K,  $\tau = 2.47 \times 10^4$  a.u., and  $P = 100$ . The mass of a carbon atom is  $2.2054 \times 10^4$  a.u.

fullerene to the final configuration containing a SW defect. Tersoff's empirical interatomic potential<sup>22</sup> is used. We have generated four different initial trajectories by assigning random sets of  $\{\mathbf{a}_k\}$  with a separately chosen maximum amplitude of  $A_{max}$ . Using these initial trajectories, the Passerone and Parrinello's action  $\Theta$  is minimized. We find that, although the total energies are well conserved for all cases, the final converged trajectories are quite sensitive to the initial assignment of  $\{\mathbf{a}_k\}$ , and they are significantly different from each other. Consequently, the kinetic energy, the potential and kinetic-energy fluctuations, and the value of the Onsager-Machlup action  $O$  are quite different from trajectory to trajectory. The results are summarized in Table I. The kinetic energy of each atom along the final converged trajectory is averaged. We find that the time-averaged kinetic energy fluctuates quite significantly from atom to atom. These fluctuations are also shown in Table I. This large kinetic energy fluctuation is intuitively undesirable and it would be quite useful if one can introduce a procedure which assigns an appropriate value of kinetic energy to all atoms in the system so that the kinetic-energy fluctuates significantly less than compared to the cases of the four trajectories above (see

Table I). In this work, by introducing such a procedure of kinetic-energy control, we demonstrate that the quality of the resulting trajectories is significantly improved compared to the original ADMD results.

In order to control the kinetic energy of each atom, we introduce an additional penalty term to the Passerone and Parrinello's action and the extended action  $\tilde{\Theta}$  becomes

$$\tilde{\Theta}(\{\mathbf{R}_j\}, E; T) = \Theta(\{\mathbf{R}_j\}, E) + \nu \sum_{I=1}^N \left( \langle K_I \rangle - \frac{3k_B T}{2} \right)^2, \quad (4)$$

where  $K_I = M_I(\mathbf{R}_j^I - \mathbf{R}_{j+1}^I)^2 / (2\Delta^2)$  is the instantaneous kinetic energy of the atom  $I$  at time step  $j$ ,  $\langle K_I \rangle$  is its time-average value over the entire trajectory ( $P$  steps),  $T$  is the target temperature of the system which we set, and  $k_B$  is the Boltzmann's constant. The parameter  $\nu$  controls the strength of the kinetic energy enforcement to the value corresponding to the target temperature.



TABLE I. Fictitious temperatures  $T'$  defined by  $\sum_{l=1}^N \langle K_l \rangle = 3Nk_B T'/2$ , the atomic fluctuation of  $T'$  ( $\Delta T'$ ), and  $O$  (discretized Onsager-Machlup action) are evaluated for four different ADMD simulations starting from random sets of sine expansion coefficients with maximum amplitude  $A_{max}$ . Here we use  $\mu = 10^8$  a.u.,  $\nu = 10^{10}$  a.u.,  $E = -14.6$  a.u., target variable  $T = 500$  K,  $\tau = 2.47 \times 10^4$  a.u., and  $P = 100$ . The mass of a carbon atom is  $2.2054 \times 10^4$  a.u.

	$A_{max}$ (a.u.)	$T'$ (K)	$\Delta T'$ (K)	$O$ (a.u.)
Original	0.3	114.3	69.3	113.5
ADMD results	0.1	64.9	49.6	180.0
with $\Theta(\{\mathbf{R}_j\}, E)$	0.01	52.8	72.3	217.8
	0.001	55.2	114.9	208.6
Proposed	0.3	499.5	0.0	21.6
ADMD results	0.1	499.7	0.0	23.7
with $\tilde{\Theta}(\{\mathbf{R}_j\}, E; T)$	0.01	499.7	0.0	17.5
	0.001	499.5	0.0	39.2

With the proposed action  $\tilde{\Theta}$  to be minimized, we repeated the ADMD simulations using the same initial assignment of  $\{\mathbf{a}_k\}$  as above. We have used the target temperature  $T = 500$  K and  $\nu = 10^{10}$  a.u., and the results are summarized in the lower panel of Table I. The total-energy conservation is as well established as in the original ADMD simulations. Compared to the original ADMD simulation results of the four separate cases above, the final converged trajectories are relatively similar to each other representing insensitivity of the initial assignment of  $\{\mathbf{a}_k\}$  in the case of the proposed approach. When we measure the Onsager-Machlup action  $O$ , we find that the quality of the paths from the proposed extended action is significantly improved (see Table I). Apart from the fact that the time-averaged kinetic energy has little fluctuation (due to the newly introduced penalty term), we observe that the fluctuation of  $O$ , from the variation of the random initial trajectories, is also reduced.

In Fig. 2, we plot the distribution of the components of the vector  $\{2\mathbf{R}_j^l - \mathbf{R}_{j-1}^l - \mathbf{R}_{j+1}^l - (\Delta^2/M_l)[\partial V(\{\mathbf{R}_j\})/\partial \mathbf{R}_j^l]\}$  collected from the final converged trajectories from both the present and the original ADMD simulations. We find that the data fit well to Gaussian distributions for both ADMD results. Apparently, the width of the distribution from the present method is smaller than that from the original method representing that the present method provides atomic trajectories of better-quality.

To demonstrate the details of the difference between the results of the original and the proposed ADMD simulations we show in Fig. 1 two final converged paths obtained from the two simulations on the SW-defect formation in  $C_{60}$ . We first focus on the path of one of the two carbon atoms directly involved in the SW defect. The path from the present method fluctuates less in space than that from the original Passerone and Parrinello's method. In Fig. 1, the SW defect is created approximately during the time interval of  $40 < j < 60$ , where overall repositioning of the atom occurs. The definition of this time interval is less clear in the case of the original ADMD simulation. When we plot the potential en-

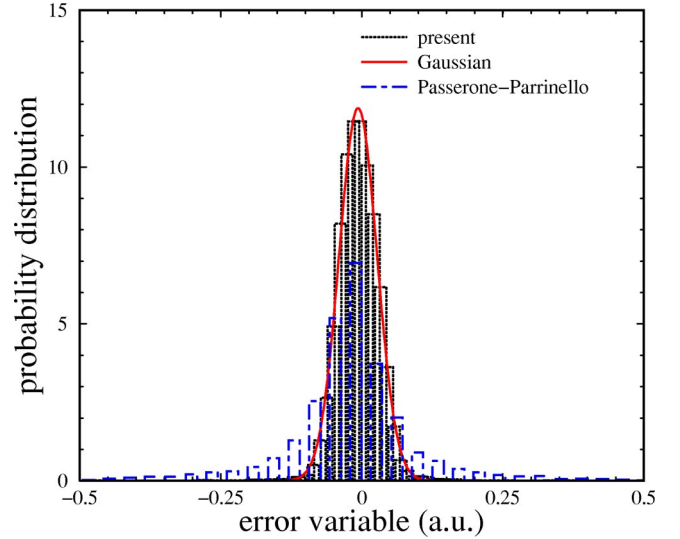


FIG. 2. A typical distribution of the scalar error variables is shown. Calculated distribution of the scalar error variables from the vectors  $\{2\mathbf{R}_j^l - \mathbf{R}_{j-1}^l - \mathbf{R}_{j+1}^l - (\Delta^2/M_l)[\partial V(\{\mathbf{R}_j\})/\partial \mathbf{R}_j^l]\}$ , obtained from the present ADMD method is shown in dotted bars. It fits well with a Gaussian distribution function as shown by a solid line. Dot-dashed bars represent the distribution of the scalar error variables obtained from the Passerone and Parrinello's original ADMD method. In the limit where the width of the Gaussian distribution is infinitesimal, we expect an exact Verlet trajectory that would have been generated by the Verlet algorithm solving Newton's equations of motion.

ergy versus the time step, the value of the potential energy of the system is much lower before and after the formation of the SW defect in the present method. On the other hand, in the case of the original ADMD simulation, the potential-energy fluctuates around a high value throughout the entire path. This clearly demonstrates the qualitative difference between the two trajectories. In the original ADMD simulation, the system wanders through many high potential-energy states (i.e., at least one of the chemical bonds connected to the two SW-defect atoms is broken in the early stages of the simulation and remains in a broken-bond state almost until the end). In the present method, the SW-defect atom remains near the given initial position with relatively low potential energy and it relocates its overall position during the time interval of  $40 < j < 60$  gently crossing over the activation energy barrier. It is interesting to observe that, in the simulations from the proposed method, collective kinetic-energy transfer occurs between the two SW-defect atoms and the rest of the 58 atoms near the beginning and the end of the defect formation.

In the present method, the positions of the two SW-defect carbons fluctuate much less compared to the original ADMD results. In addition, due to the constraint of the time-averaged kinetic energy of the SW-defect atoms, the contribution of the kinetic energy from the outside of the the SW-defect forming interval is relatively small compared to the contribution from the SW-defect forming interval, where the mandatory motion of the defect formation occurs. On the other hand, the motion of the other 58 atoms is more (less)

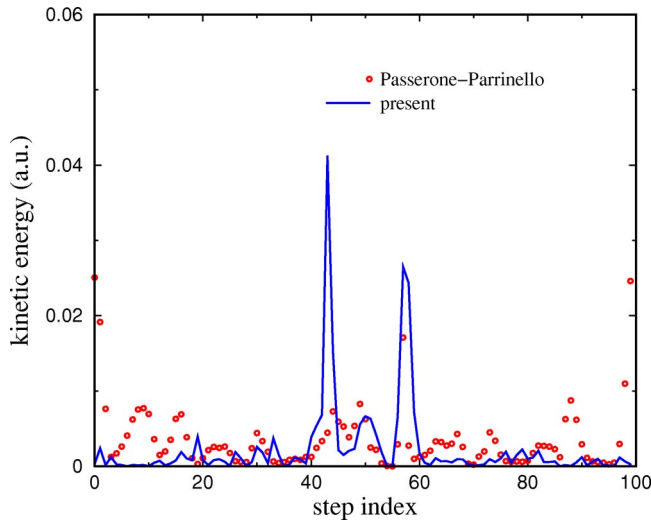


FIG. 3. The kinetic energy of one of the two SW-defect atoms is shown along the paths of the original ADMD simulation and the proposed ADMD results. The SW-defect is formed around the step index  $40 \leq j \leq 60$  for both cases. We observe that, for the case of the current approach, the kinetic energy of an SW-defect atom is markedly higher in the SW-defect forming interval while it is lower outside the interval. The distribution of kinetic energy of the other 58 atoms acts in a opposite fashion, i.e., high kinetic energy outside and low kinetic energy inside (data not shown). On the other hand, the kinetic energy distribution from the original ADMD simulation does not show such time step index dependency or atomic site dependency.

active outside (inside) the SW-defect forming interval. This is in marked contrast to the case of the original ADMD results where the kinetic energy of most 60 atoms fluctuate wildly for the entire trajectory. In Fig. 3, we plot the kinetic energy of a SW-defect atom along the paths of the original ADMD simulation and the proposed ADMD results.

It should be noted that, when a path is converged, the contribution of the kinetic-energy control term to the object function  $\tilde{\Theta}(\{\mathbf{R}_j\}, E; T)$  is negligible (typically  $\sim 0.1\%$ ). This means that the path obtained from the proposed approach also serves as a solution to the original Passerone and Parrinello's ADMD method only with much improved path quality measured by the smaller value of Onsager-Machlup action  $O$ .

In principle, one can employ two stages of computation. In the first stage, one uses the proposed extended action  $\tilde{\Theta}(\{\mathbf{R}_j\}, E; T)$  for ADMD simulations. In the second stage, one switches to the original Passerone and Parrinello's action  $\Theta(\{\mathbf{R}_j\}, E)$ , where the final converged result of  $\{\mathbf{a}_k\}$  obtained from the first stage is used as an input. We have experimented this two stage procedure in several cases, and we find that the difference between the final trajectories from the first stage and the second stage is minimal.

One technical aspect of the proposed approach is to determine the appropriate values of the target temperature  $T$  and the parameter  $\nu$ . In the original ADMD method, the values of the total energy  $E$  and the parameter  $\mu$  can be set to an appropriate value.<sup>5</sup> Once the values of  $E$  and  $\mu$  are set,

and the values of potential energy are evaluated at the given initial and final configurations of a system, several values of  $T$  can be tried. Typically, the kinetic energy is bounded by the energy difference between the total energy  $E$  and the potential-energy value of either the initial or the final configuration. Regarding to the parameter  $\nu$ , we have tried several values in the range between  $10^8$  and  $10^{11}$  a.u. We find that the results are insensitive to the particular choice of  $\nu$ . It should be noted that the target temperature  $T$  is only a parameter to control the time-averaged kinetic energy in ADMD simulations, and we do not intend to interpret it as a physical quantity.

## B. One-way multigrid method

Direct application of the conjugate gradient method<sup>23</sup> to a trajectory containing high-frequency components of the sine expansion coefficients is not an efficient approach for action minimization since slowly varying low-frequency components of the trial trajectory do not converge well. Therefore, when performing path relaxation, it is convenient to start with a path containing low-frequency components only and move on by gradually adding higher frequency components to the path to accelerate the convergence.<sup>5</sup>

It should be noted that very high-frequency components of the sine expansion of the final converged trajectory are typically quite small, whereas the amplitudes of low-frequency components are large. For example, we consider the fusion process of two  $C_{60}$  molecules into a  $C_{120}$  carbon capsule molecule as shown in Fig. 4. We choose the chirality of the capsule as that of the (5,5) carbon nanotube. In the simulation, we place two  $C_{60}$  molecules separated by 9.9 Å (center to center) as shown in the figure. Before applying the ADMD simulation, the potential energies of initial and final configurations are separately minimized by conjugate gradient minimization method,<sup>23</sup> so that each of them corresponds to the most stable structure of its potential-energy basin.

The ADMD simulation of the  $C_{120}$  fusion process is quite a nontrivial example of complicated kinetic configurational rearrangement, since it involves many Stone-Wales-type<sup>19</sup> bond rotations. In Fig. 4, we show a typical Fourier components of the final path. We find that the low-frequency components of  $\{\mathbf{a}_k\}$  fluctuate much from atom to atom, while the amplitudes of high-frequency components are all quite small. This indicates that the multigrid method is efficient for obtaining good final converged trajectories.<sup>23,24</sup>

The object function minimization is carried out on several levels of accuracy defined by the ever-increasing number of the sine expansion coefficients  $\{\mathbf{a}_k\}$  as typically performed in the one-way multigrid electronic structure calculations.<sup>24</sup> We have used seven (arbitrary number) levels of accuracy and applied the conjugate gradient minimization method<sup>23</sup> at each level. The output of a lower level calculation is iteratively used as the input for the next-level calculation (after the addition of higher frequency components of  $\{\mathbf{a}_k\}$ ) following the one-way multigrid schedule. During the multigrid calculation, the number of configurations,  $P$  is fixed.

A typical convergence plot of the value of the object function  $\tilde{\Theta}$  during the one-way multigrid minimization procedure

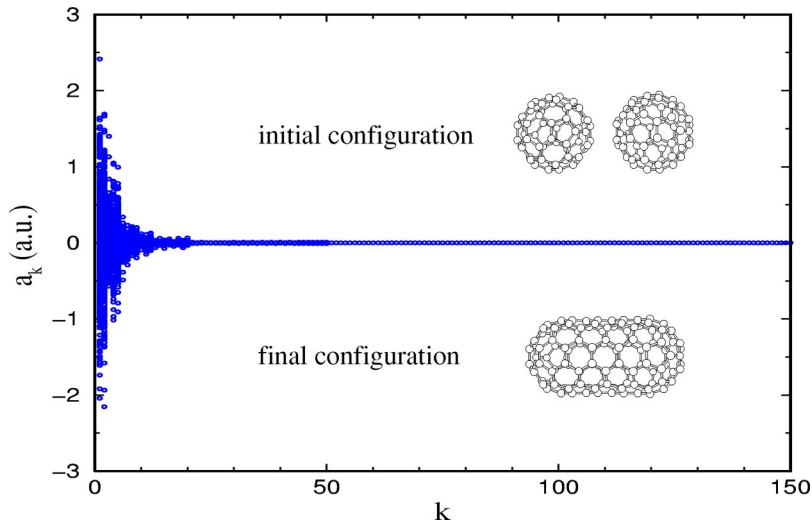


FIG. 4. The scalar components of  $\mathbf{a}_k$  are shown for the final converged path obtained by the current ADMD simulation. The system under investigation is the fusion process of two  $C_{60}$  molecules into a carbon capsule  $C_{120}$ . The importance of the slowly varying components in the atomic path construction is illustrated. We observe large variation of sine expansion coefficients at the low-frequency regime.

is shown in Fig. 5. The three components of the action, the discretized classical action and the two penalty function terms are shown in the figure. In addition, we have evaluated the discretized Onsager-Machlup action  $O$ . We observe that the values of the total energy and the time-averaged kinetic energy rapidly approach to their pre-assigned values in the early stages of simulations, indicating the numerical stability of the proposed ADMD method. When a path is converged by the minimization procedure the contribution of the second penalty term (kinetic-energy control term) to the value of the total object function is minimal. This demonstrates that the proposed ADMD approach can identify a satisfactory (in terms of the small value of  $O$ ) trajectory from many possible trajectories which one would have obtained following the original version of ADMD simulation by Passerone and Parrinello, and the path relaxation procedure utilizing the proposed extended action can be thought as a trajectory annealing.

In a practical calculation of an atomic trajectory, one needs a procedure to assign the path of each atom of the system under consideration, from the initial to the final configuration. Especially, when dealing with identical particles (as in the  $C_{60}$  and  $C_{120}$  systems), there is a set of free parameters associated with the relative translational and rotational degrees of freedom between the initial and final configurations. We have used the least-square superposition of two atomic coordinate sets via quaternion method.<sup>25</sup> The first coordinate set is fixed while the second one is translated and rotated to provide the best fit. In complex cases, we introduce an atomic index exchange procedure prior to the ADMD simulation to best superpose the initial atomic positions to the final ones. For this purpose, we used a simulated annealing method.<sup>17</sup>

### C. Action-derived molecular dynamics and nudged elastic band method

Here we compare the results of the proposed ADMD simulations and the nudged elastic band method<sup>6</sup> for the structural rearrangement of two  $C_{60}$  molecules into a carbon capsule  $C_{120}$ , as discussed above.<sup>26</sup> Figure 6 shows the val-

ues of the potential energy along the trajectories obtained from the two methods. When we examine the trajectories obtained from the nudged elastic band method, we find that several Stone-Wales-type bond rotations occur simultaneously. Consequently, the configuration of the highest potential-energy state (near step index 70) contains many carbons with coordination number less than three (i.e., these carbons have broken chemical bonds), and the estimated activation energy is about 40.8 eV. In the practical application of the nudged elastic band method to a complex system, such as the carbon capsule  $C_{120}$  formation from two  $C_{60}$  mol-

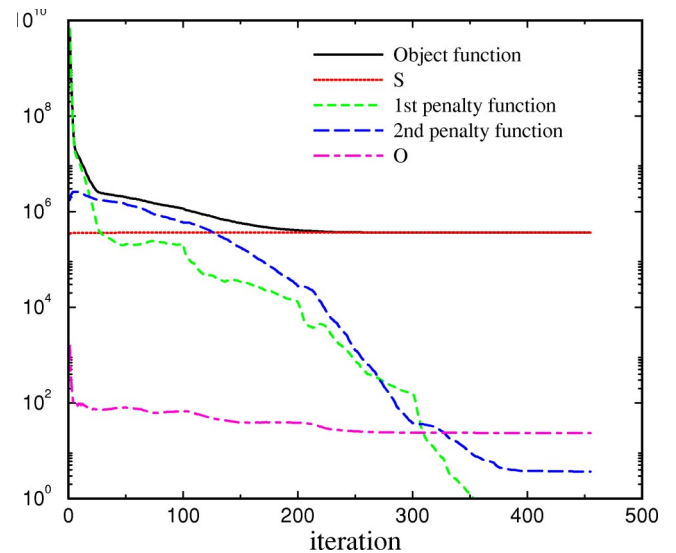


FIG. 5. Convergence characteristics of various quantities during a typical minimization process of the extended action  $\tilde{\Theta}$  is shown. Atomic units are used for the vertical axis. The object function consists of three terms, a discretized action  $S$  and two penalty function terms for total and kinetic energy controls. The contribution of the second penalty term to the object function is minimal (less than 0.1%) when the trajectories are converged. We use  $\mu = 10^8$  a.u.,  $\nu = 10^{10}$  a.u.,  $E = -14.6$  a.u.,  $T = 500$  K,  $\tau = 2.47 \times 10^4$  a.u.,  $P = 100$ , and  $A_{max} = 0.1$  a.u. The mass of a carbon atom is  $2.2054 \times 10^4$  a.u.



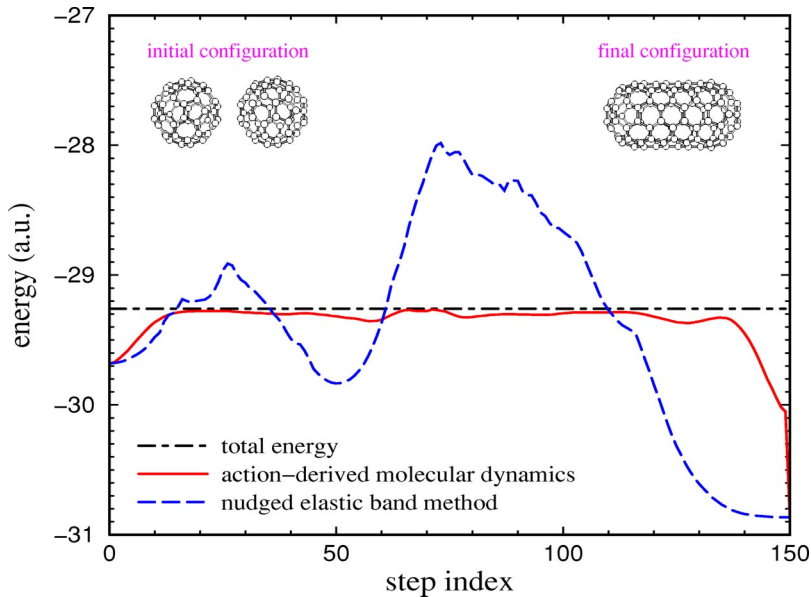


FIG. 6. The results of the ADMD method and the nudged elastic band method are compared for the fusion reaction of two  $C_{60}$  molecules into a  $C_{120}$  molecule. Potential-energy fluctuations along the two trajectories are shown. It should be noted that in the ADMD simulation, the value of the total energy is controlled to the value indicated by the horizontal line in the figure. For ADMD simulation, we use  $\mu=10^8$  a.u.,  $\nu=10^{10}$  a.u.,  $E=-29.44$  a.u.,  $T=200$  K,  $\tau=3.71\times 10^4$  a.u., and  $P=150$ . For nudged elastic band simulation, we use  $\tau=3.71\times 10^4$  a.u., and  $P=150$ . The mass of a carbon atom is  $2.2054\times 10^4$  a.u. The same initial guess of the trajectories is used for the two simulations. The initial and final atomic configurations are shown at the left and right corners, respectively. Tersoff's empirical interatomic potential is used.

ecules, one has to repeatedly obtain many trajectories while varying the initial assignment of  $\{\mathbf{a}_k\}$ .<sup>6</sup> In Fig. 6, we show the best nudged elastic band results from our ten independent calculations (i.e., the one with the least value of activation energy barrier).

On the other hand, in the application of ADMD simulations, one can avoid high potential-energy configurations, by assigning an appropriate value of target total energy. Consequently, the trajectory from the present ADMD simulation involves a series of Stone-Wales-type bond rotations one after another, keeping the number of under-coordinated carbons at a minimal value. The activation energy barrier estimated from the present ADMD method is about 6.2 eV. Since the major aim of the study of rare events is to find the most probable transition state (i.e., the lowest energy saddle point connecting the given initial and final states), this clearly demonstrates that the ADMD method is more efficient than the nudged elastic band method in correctly estimating the activation energy barrier. We find that, in simple cases, the nudged elastic band method works as well as the ADMD. For complicated systems, the nudged elastic band method typically overestimates the activation energy barrier.

#### D. Parallel computational aspect of ADMD

One of the advantage of the ADMD method is that its calculation can be easily and efficiently parallelized. At each path relaxation step in the object function minimization procedure, one has to evaluate the potential-energy function and the atomic forces for  $P-1$  independent configurations. Since these  $P-1$  calculations are the most time consuming part of the ADMD simulation, and since they are completely independent of each other, one can easily take advantage of parallel computation with high parallel efficiency. The CPU time associated with the relaxation of the path is minimal compared to that of potential energy and atomic forces evaluation. This is due to the characteristic parallel-

computation-friendly coordinate discretization of the ADMD simulation in contrast to the opposite case in ordinary molecular dynamics.

#### IV. CONCLUSIONS

The ADMD simulation is a powerful method for the study of rare events for given initial and final configurations, while ordinary molecular dynamic approaches would take astronomical amounts of computational resources to overcome large activation energy barrier between them. We have proposed an extended action for the ADMD simulation that consists of three terms, a discretized classical action and two penalty function terms to control both the total energy and the time-averaged kinetic energy of each atom.

The quality of atomic trajectories obtained by the proposed ADMD method is significantly improved in terms of the smaller value of Onsager-Machlup action compared to that from the original ADMD method. The proposed action is useful for improving path quality and can be used as an atomic trajectory annealing method. This feature was demonstrated by the fact that the path from the proposed ADMD method is also a solution of the original method by Passerone and Parrinello, the difference being only the smaller value of the Onsager-Machlup action. We found that ADMD is superior to the nudged elastic band in finding low activation energy barrier between two given states of a complex system.

The ADMD calculation can be easily and efficiently processed by parallel computation indicating that the method is useful for studying pathways of complex systems. The implementation of the proposed approach to a general system is quite straightforward as in the case of ordinary molecular dynamics simulations, since the only requirement is to evaluate the potential energy and the atomic forces.

#### ACKNOWLEDGMENTS

The authors gratefully acknowledge stimulating and helpful discussions with D. Passerone and M. Parrinello. This

work was supported by The Swiss-Korean Outstanding Research Efforts Award Program of the Ministry of Science and Technology and The 4th Supercomputing Application Support Program of the Korea Institute of Science and Technol-

ogy Information. I.H.L. acknowledges support by the Ministry of Science and Technology of Korea through the National Science and Technology Program, Grant No. M1-0213-04-0002.

\*Electronic address: ihlee@kriss.re.kr

<sup>1</sup>M. P. Allen and D. J. Tildesley, *Computer Simulation of Liquids* (Oxford University Press Inc., New York, 1987).

<sup>2</sup>R. E. Gillilan and K. R. Wilson, *J. Chem. Phys.* **97**, 1757 (1992).

<sup>3</sup>R. Olender and R. Elber, *J. Chem. Phys.* **105**, 9299 (1996).

<sup>4</sup>C. Dellago, P. G. Bolhuis, F. S. Csajka, and D. Chandler, *J. Chem. Phys.* **108**, 1964 (1998).

<sup>5</sup>D. Passerone and M. Parrinello, *Phys. Rev. Lett.* **87**, 108302 (2001); D. Passerone, M. Ceccarelli, and M. Parrinello, *J. Chem. Phys.* **118**, 2025 (2003).

<sup>6</sup>H. Jónsson, G. Mills, and K. W. Jacobsen, in *Computer Simulation of Rare Events and Dynamics of Classical and Quantum Condensed-Phase Systems-Classical and Quantum Dynamics in Condensed Phase Simulations*, edited by B. J. Berne, G. Cicotti, and D. Coker (World Scientific, Singapore, 1998).

<sup>7</sup>W. E. W. Ren, and E. Vanden-Eijnden, *Phys. Rev. B* **66**, 052301 (2002).

<sup>8</sup>G. T. Barkema and N. Mousseau, *Phys. Rev. Lett.* **77**, 4358 (1996).

<sup>9</sup>A. F. Voter, *Phys. Rev. Lett.* **78**, 3908 (1997).

<sup>10</sup>V. Zaloz and R. Elber, *Comput. Phys. Commun.* **128**, 118 (2000).

<sup>11</sup>A. F. Voter, *Phys. Rev. B* **57**, R13 985 (1998).

<sup>12</sup>G. Henkelman and H. Jónsson, *J. Chem. Phys.* **111**, 7010 (1999).

<sup>13</sup>G. Henkelman and H. Jónsson, *J. Chem. Phys.* **115**, 9657 (2001).

<sup>14</sup>J. D. Doll, T. L. Beck, and D. L. Freeman, *Int. J. Quantum Chem., Quantum Chem. Symp.* **23**, 73 (1989).

<sup>15</sup>A. E. Cho, J. D. Doll, and D. L. Freeman, *Chem. Phys. Lett.* **229**, 218 (1994).

<sup>16</sup>D. Passerone and M. Parrinello (private communications).

<sup>17</sup>S. Kirkpatrick, C. D. Gelatt, and M. P. Vecchi, *Science* **220**, 671 (1983).

<sup>18</sup>L. Verlet, *Phys. Rev.* **159**, 98 (1967).

<sup>19</sup>A. J. Stone and D. J. Wales, *Chem. Phys. Lett.* **128**, 501 (1986).

<sup>20</sup>J.-Y. Yi and J. Bernholc, *J. Chem. Phys.* **96**, 8634 (1992).

<sup>21</sup>P. A. Marcos, M. J. López, A. Rubio, and J. A. Alonso, *Chem. Phys. Lett.* **273**, 367 (1997).

<sup>22</sup>J. Tersoff, *Phys. Rev. Lett.* **61**, 2879 (1988).

<sup>23</sup>W. H. Press, S. A. Teukolsky, W. T. Vetterling, and B. P. Flannery, *Numerical Recipes in Fortran, The Art of Scientific Computing*, 2nd Edition (Cambridge University Press, Cambridge, England, 1992).

<sup>24</sup>I.-H. Lee, Y.-H. Kim, and R. M. Martin, *Phys. Rev. B* **61**, 4397 (2000).

<sup>25</sup>S. J. Kearsley, *J. Comput. Chem.* **11**, 1187 (1990).

<sup>26</sup>B. W. Smith, M. Monthieux, and D. E. Luzzi, *Chem. Phys. Lett.* **315**, 31 (1999); B. W. Smith and D. E. Luzzi, *ibid.* **321**, 169 (2000).